Biosensors and Bioelectronics ▮ (▮▮▮▮) ▮▮▮–▮▮▮

Contents lists available at SciVerse ScienceDirect

Biosensors and Bioelectronics

journal homepage: www.elsevier.com/locate/bios

Biomimetic sensor for certain catecholamines employing copper(II) complex and silver nanoparticle modified glassy carbon paste electrode

Bankim J. Sanghavi [a], Shaikh M. Mobin [a,b,c], Pradeep Mathur [b,c], Goutam K. Lahiri [b,c], Ashwini K. Srivastava [a,*]

[a] Department of Chemistry, University of Mumbai, Vidyanagari, Mumbai 400098, India
[b] National Single Crystal X-ray Diffraction Facility, IIT Bombay, Powai, Mumbai 400076, India
[c] Department of Chemistry, IIT Bombay, Powai, Mumbai 400076, India

ARTICLE INFO

Article history:
Received 7 May 2012
Received in revised form
2 July 2012
Accepted 6 July 2012

Keywords:
Biomimetic sensor
Catecholamines
Copper complex
Silver nanoparticles
Glassy carbon paste electrode
Adsorptive stripping voltammetry

ABSTRACT

A dimeric Cu(II) complex $[Cu(\mu_2\text{-hep})(\text{hep-H})]_2 \cdot 2ClO_4$ (**1**) containing bidentate (hep-*H*=2-(2-hydroxyethyl)pyridine) ligand was synthesized and characterized by single crystal X-ray diffraction studies. Each Cu-ion in **1** is in a distorted square pyramidal geometry. Further **1** along with silver nanoparticles (SNPs) have been used as modifier in the construction of a biomimetic sensor (**1**–SNP–GCPE) for determining certain catecholamines viz., dopamine (DA), levodopa (L-Dopa), epinephrine (EP) and norepinephrine (NE) using cyclic voltammetry, chronocoulometry, electrochemical impedance spectroscopy and adsorptive stripping square wave voltammetry (AdSSWV). Finally, the catalytic properties of the sensor were characterized by chronoamperometry. Employing AdSSWV, the calibration curves showed linear response ranging between 10^{-6} and 10^{-9} M for all the four analytes with detection limits ($S/N=3$) of 8.52×10^{-10} M, 2.41×10^{-9} M, 3.96×10^{-10} M and 3.54×10^{-10} M for DA, L-Dopa, EP and NE respectively. The lifetime of the biomimetic sensor was 3 months at room temperature. The prepared modified electrode shows several advantages such as simple preparation method, high sensitivity, high stability, ease of preparation and regeneration of the electrode surface by simple polishing along with excellent reproducibility. The method has been applied for the selective and precise analysis of DA, L-Dopa, EP and NE in pharmaceutical formulations, urine and blood serum samples.

© 2012 Elsevier B.V. All rights reserved.

1. Introduction

Catecholamines [viz., dopamine (DA), levodopa (L-Dopa), epinephrine (EP) and norepinephrine (NE)] play a significant role in the nervous system as central and peripheral neurotransmitters. They are biological amines released mainly from the adrenal glands in response to stress. They act as neurotransmitters (except L-Dopa which is a precursor to DA), thus maintaining normal physical activity of the body including heart rate, blood pressure and the reactions of the sympathetic nervous system (Kumar et al., 2011). Very high levels of catecholamines in biological fluids indicate neural tumors and/or tumors of adrenal glands (Barron, 2010; Castleberry, 1997). The determination of catecholamines in biological fluids is of great importance in medical diagnostics, especially for patients suffering from Parkinson's disease and stress. Therefore, there is a need for their quantitative determination in biological fluids for detecting any endocrine disorders or any other physiological and pathological abnormality in the body (Whiting, 2009).

There are some methods applied for the determination of catecholamines such as high performance liquid chromatography (Chirita et al., 2010; Chirita et al., 2011) capillary electrophoresis (Claude et al., 2011; Zhao et al., 2011), LC–MS/MS (Van De Merbel et al., 2011), chemiluminescence (Li et al., 2011a, 2011b) and fluorescence detection (Diao et al., 2011).However, most of these methods are complicated as they need derivatization procedures or combination of various detection methods. Moreover, some of them suffer from low sensitivity and selectivity in the corresponding determinations. In comparison, electrochemical detection methods have shown remarkable advantages such as high sensitivity, low cost and simple surface modification of electrodes. Moreover, they are not as time consuming as the chromatographic methods. As a result of these advantages, a variety of electrochemical methods are available for the determination of DA (Deng et al., 2011; Huang et al., 2011; Jia et al., 2011; Li et al., 2011a, 2011b; Noroozifar et al., 2011), L-Dopa (Babaei and Babazadeh, 2011a, 2011b; Hu et al., 2010; Mathiyarasu and Nyholm, 2010; Mazloum-Ardakani et al., 2011a), EP (Goyal and

* Corresponding author. Fax: +91 22 26526119.
E-mail addresses: aksrivastava@chem.mu.ac.in, akschbu@yahoo.com (A.K. Srivastava).

0956-5663/$ - see front matter © 2012 Elsevier B.V. All rights reserved.
http://dx.doi.org/10.1016/j.bios.2012.07.008

Bishnoi, 2011; Goyal et al., 2011; Lu et al., 2011; Mazloum-Ardakani et al., 2011b; Shahrokhian and Khafaji, 2010) and NE (Beitollahi and Sheikhshoaie, 2011; da Silva et al., 2011; Goyal and Bishnoi, 2011; Huang et al., 2010; Mazloum-Ardakani et al., 2010)

Electrochemical analysis based on chemically modified electrodes (CMEs) has proved to be a sensitive and selective method for the determination of various organic molecules (Ensafi et al., 2010; Zima et al., 2009) as well as metal ions (Švancara et al., 2009). These electrodes are inexpensive and possess many advantages such as low background current, wide range of potential windows, rapid surface renewal and easy fabrication. Nanomaterials (Sanghavi and Srivastava, 2010; Sanghavi and Srivastava, 2011a, 2011b; Gadhari et al., 2010; Sanghavi et al., 2012), macrocycles (Vaze and Srivastava, 2007; Kotkar et al., 2007), rice husk (Gadhari et al., 2011), etc. are some of the modifiers employed to fabricate CMEs.

A Cu(II) complex based biomimetic sensor is a developing area in current research based on sensors. An up-to-date literature survey reveals that a few Cu(II) complex based biomimetic sensors have been employed for the trace determination of dihydroxy molecules due to their redox properties (de Carvalho et al., 2008; Fernandes et al., 2010; Lakshmi et al., 2009; Sotomayor et al., 2003a, 2003b; Shaikh et al., 2010). Silver nanoparticles, on the other hand, exhibit high electrocatalytic activity towards the compounds which have sluggish redox process at bare electrodes (Encarnación Burgoa Calvo et al., 2007; Lin et al., 2008). Therefore, a synergistic effect of both copper(II) complex and silver nanoparticles can lead to a highly sensitive method for catecholamines determination.

In present study, copper(II) complex (**1**) and silver nanoparticles (SNP) modified glassy carbon-paste electrode (**1**–SNP–GCPE) was constructed and used for determination of DA, L-Dopa, EP and NE. The electrochemical behavior of these species at the **1**–SNP–GCPE was investigated using cyclic voltammetry (CV), electrochemical impedance spectroscopy (EIS), chronocoulometry (CC) and adsorptive stripping square wave voltammetry (AdSSWV) techniques. Based on the different electrocatalytic activities of the modified electrode towards DA, L-Dopa, EP and NE, the sensitive and selective methods for their determination were established. The detection of these catecholamines in urine, human serum was finally demonstrated as real sample applications.

2. Materials and methods

2.1. Chemicals and instrumentation

All chemicals were of A.R. grade and were used as received without any further purification. DA, L-Dopa, EP and NE were procured from Sigma Aldrich. SNPs (<100 nm, 99.5%) were obtained from Aldrich (USA). The commercially available starting materials, $Cu(OC(=O)CH_3)_2\cdot 2H_2O$, 2-(2-hydroxyethyl)pyridine (hep-H), sodium perchlorate ($NaClO_4$) and reagent grade solvent methanol, were used as received. Glassy carbon powder was purchased from Aldrich. All solutions were prepared using double distilled water of specific conductivity (0.3–0.8 μS). The developed method was employed for analysis of the following pharmaceuticals: Dopar, Intropin (both brands contain 4 mg/mL DA), Elcepam, Sinemet (both brands contain 100 mg/ tablet L-Dopa), Adrenaline injection, Q-Med (both brands contain 1 mg/mL EP) and Adrenor, Adrenerz injection (both brands contain 2 mg/mL NE). All these catecholamines were also determined in human urine and blood serum samples.

All Voltammetric, Chrono and Electrochemical Impedance Spectroscopic (EIS) measurements have been performed on Eco Chemie, Electrochemical Work Station, model Autolab PGSTAT 30 using GPES software, version 4.9.005 and Frequency Response Analyser, software version 2.0 respectively. A conventional three electrode system was used with a glassy carbon paste electrode (unmodified or modified) as a working electrode, a saturated Ag/AgCl reference electrode and a Pt wire counter electrode. All pH measurements were performed using ELICO LI 127 pH meter. Elemental analyses were carried out with a Perkin-Elmer 240C elemental analyzer. FT-IR spectra of complexes as KBr pellets were recorded using Nicolet spectrophotometer. HPLC used for validating the method was an Agilent model 1100. The scanning electron microscope employed for surface characterization of the electrodes was a FEI Quanta-200 model with an operating voltage of 20 kV.

2.2. Synthesis of $[Cu(\mu_2\text{-hep})(\text{hep-H})]_2\cdot 2ClO_4$ (**1**)

A solution of hep-H (123 mg, 1 mmol) in methanol (25 mL) was added to a solution of $Cu(OC(=O)CH_3)_2\cdot 2H_2O$ (199 mg, 1 mmol) in methanol (25 mL). An aqueous solution of $NaClO_4$ (123 mg, 1 mmol) was added to the above reaction mixture, and the resultant solution was stirred for 6 h at room temperature. The solution was then passed through the filter paper in order to remove any unreacted materials. The filtrate was allowed to stand at room temperature for crystallization. Dark blue single crystals of **2** were obtained within 5 days by slow evaporation of the solvent. M.P. 228–230 °C. Yield, 180 mg (90%). Anal. Calcd for $C_{28}H_{34}N_4O_4F_{12}P_2Cu_2$, ($MW$=816.58): C, 37.08; H, 3.78; N, 6.17. Found: C, 37.05; H, 3.81; N, 6.19. IR (KBr, cm^{-1}): 3460(br), 3170(w), 2355(w), 2366(w), 1629(m), 1553(w), 1489(m), 1451(s), 1322(w), 1181(w), 1173(w), 1068(s), 1052(m), 1037(w), 845(s), 782(m), 562(s).

2.3. X-ray crystallography

Single crystal X-ray structural study of **1** was performed on a CCD Oxford Diffraction XCALIBUR-S diffractometer equipped with an Oxford Instruments low-temperature attachment. Data were collected at 150(2) K using graphite-monochromoated Mo Kα radiation (λ_α=0.71073 Å). The strategy for the data collection was evaluated by using the CrysAlisPro CCD software. The data were collected by the standard 'phi-omega' scan techniques, and were scaled and reduced using CrysAlisPro RED software. The structures were solved by direct methods using SHELXS-97 and refined by full matrix least-squares with SHELXL-97, refining on F^2 (Sheldrick, 2008). The positions of all the atoms were obtained by direct methods. All non-hydrogen atoms were refined anisotropically. The remaining hydrogen atoms were placed in geometrically constrained positions and refined with isotropic temperature factors, generally $1.2U_{eq}$ of their parent atoms. All the H-bonding interactions, mean plane analyses, and molecular drawings were obtained using the program Diamond (version 3.1d). The crystal and refinement data are summarized in Table S-1, and selected bond distances and bond angles are shown in Table S-2. A detailed description of the experimental procedure is provided in the Supporting information.

3. Results and discussion

3.1. Structural aspects of **1**

The compound **1** crystallizes in the orthorhombic *Pnc2* space group, with a crystallographically imposed inversion center (Table S1). The asymmetric unit consists of one Cu atom, one hep^- ligand, one hep-H group and two half symmetric free ClO_4. The crystal structure of **1** reveals the dinuclear feature of the complex with the overall composition of one $[Cu(\mu_2\text{-hep})(\text{hep-H})]_2^{2+}$ and

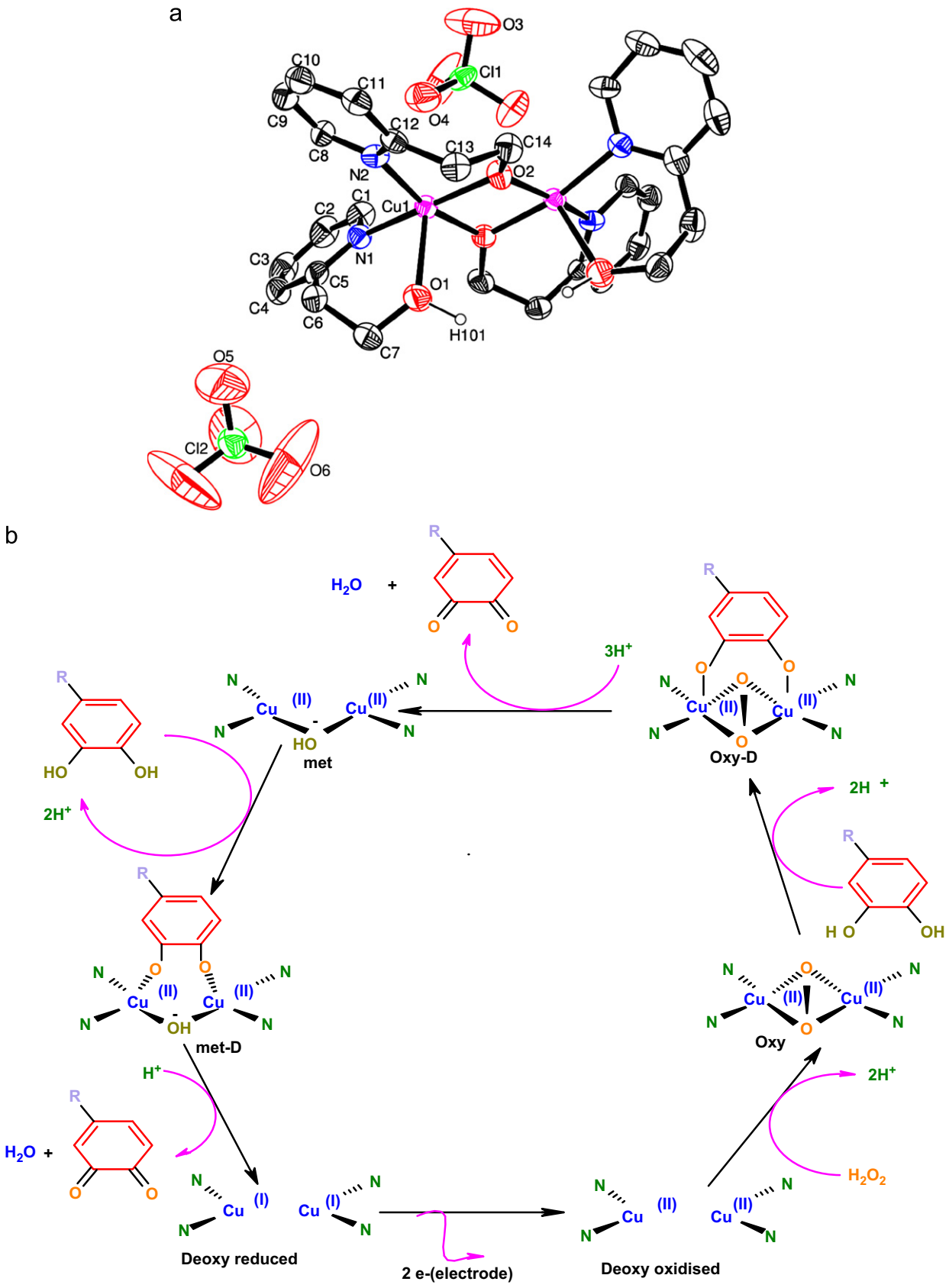

Fig. 1. (a) ORTEP view of **1** showing the molecule in the asymmetric unit with anisotropic displacement are drawn at 50% probability. (b) Mechanism for Tyrosinase in which the oxy species is formed from Cu_2^{4+} and H_2O_2. Here, D implies DOPA bound forms.

two ClO_4^- (Fig. 1(a)). Each Cu(II) ion in **1** is in a penta-coordinated N_2O_3 environment, bonded to two bridging μ-alkoxy oxygen atoms and one nitrogen atom of hep^- ligand and other nitrogen atom from hep-H ligand and the fifth coordination site is occupied by the elongated one oxygen atom of unprotonated hep-H ligand.

Please cite this article as: Sanghavi, B.J., et al., Biosensors and Bioelectronics (2012), http://dx.doi.org/10.1016/j.bios.2012.07.008

The basal position of each Cu ion in **1** is composed of O(2), O(2A), N(2) of hep$^-$ and N(1) of hep-H. The Cu(1)–O(2), Cu–O(2A), Cu(1)–N(2) and Cu(1)–N(1) bond lengths are 1.918(3), 1.927(3), 2.005(5) and 2.029(5) Å respectively, (Table S2). The axial position is filled with O(1) donor of hydroxyl group of hep-H with an elongated Cu(1)–O(1) distance of 2.329(5) Å for **1**, due to Jahn–Teller effect. This results in a distorted square pyramidal geometry around each of the copper ions. The central Cu_2O_2 ring with two different types of Cu–O bond distances is non-planar unlike the similar dimeric unit reported by us recently (Shaikh et al., 2009; Shaikh et al., 2010a, 2010b) in which central Cu_2O_2 is planar. The slight bend in the Cu_2O_2 is due to the bulkier hep-H ligand compared to $^-$OAc group. Cu···Cu distance in **1** is 3.011(1) Å. **1** is analog to the one recently published by us (Shaikh et al., 2010b) except the anion here used is perchlorate instead of PF_6. We understand that due to different hydrogen bonding patterns, the complex becomes more active for catecholamine determination. Thus, it was employed in present studies and observes suitability in sensing of the catecholamines.

The packing of **1** reveals presence of inter molecular hydrogen bonding involving C–H···O and O–H···O between each ClO_4 anion and the dimeric cationic complex (Fig. S1 and Table S3). One of the ClO_4 anion is holding two dimers through O–H···O bonding and extends the chain of 1D-polymeric chain through *b*-axis while other hold dimer through C–H···O forms a chain of another 1D-chain which inter connected forming hydrogen bonded 2D-network.

3.2. Effect of pH and supporting electrolyte

The pH of the supporting electrolyte showed a significant effect on the electrochemical behavior of DA (4.79×10^{-6} M), L-Dopa (2.95×10^{-6} M), EP (6.83×10^{-6} M) and NE (5.55×10^{-6} M) at the surface of the GCPE. Square wave voltammetry (SWV) was carried out to characterize the influence of pH of the buffer solution (in the range of 2.0–9.0). The influence of the pH on the oxidation peaks currents of DA, L-Dopa, EP and NE was investigated employing Britton–Robinson (B.R.) buffer. It was observed that as the pH of the medium was gradually increased, the potential kept on shifting towards less positive values, suggesting the involvement of proton in the reaction. Over the pH range of 2.0–9.0, the peak potential (E_p) for DA, L-Dopa, EP and NE is found to be a linear function of pH. From the plot of E_p vs. pH, slopes of −0.056, −0.055, +0.052 and −0.056 V/pH were obtained for DA (Fig. S-2), L-Dopa (Fig. S-3), EP (Fig. S-4) and NE (Fig. S-5) respectively in the working pH range. These slopes reveal that an equal number of protons and electrons are involved in the reduction reactions of DA, L-Dopa, EP and NE.

It was observed that the peak current for both DA and L-Dopa was maximum at pH 6.0 (Figs. S-2 and S-3) while that for EP and NE (Figs. S-4 and S-5) at pH 7.0. Thus, these optimized pH values were employed for further studies. Various buffers, viz., phosphate, tris, Mcllavaine and acetate buffers were then employed at pH 6.0 (Fig. S-6). Out of these, pH 6.0 acetate buffer gave the best response in terms of peak current and peak shape for both the molecules and hence was employed as a supporting electrolyte for further studies. In the next step, optimization of buffer concentration was carried out by varying its concentration in the range of 0.01–0.5 M. The best peak response was observed for 0.15 M of acetate buffer and hence was used for further studies. Similarly, pH 7.0 phosphate buffer (0.1 M) was employed as the optimum supporting electrolyte for both EP and NE (Fig. S-7).

3.3. Effect of hydrogen peroxide on the peak current of catecholamines

In the proposed sensor, the prior addition of hydrogen peroxide, before the addition of catecholamine, can be explained considering the catalytic mechanism of tyrosinase from Cu_2^{4+} plus H_2O_2 (Fig. 1(b)). Fig. 2(a) shows the effect of presence and absence of hydrogen peroxide at **1**–GCPE employing 5.78×10^{-7} M DA. In the absence of H_2O_2 a weak electrochemical signal was observed, while in the presence of H_2O_2 a good response for dopamine was obtained, suggesting that the peroxide is essential in the sensor response. Thus, the effect of varying the peroxide concentration from 0.0 to 3.0×10^{-4} M in pH 6 acetate buffer on the sensor response was examined (Fig. 2(b)). In the range studied, the analytical response increases with an increase in the concentration of the hydrogen peroxide solution up to 1.5×10^{-4} M and then leveled off. Similar results were obtained in case of L-Dopa, EP and NE. Therefore, a hydrogen peroxide concentration of 1.5×10^{-4} M was used for further studies.

The mechanism for the interaction between **1** and catecholamines in the presence of H_2O_2 is as presented in Fig.1(b) (Sotomayor et al., 2003a, 2003b). In the presence of catecholamine, a series of H^+ exchanges occur resulting in an oxygen insertion into the phenolic ring and electron donation from the copper atoms giving rise to o-quinone, water and deoxy reduced form, which is then oxidized to generate the Cu_2^{4+} form, by applying an adequate potential, in order to bind the new peroxide. This mechanism is based on the tyrosinase active site. In the first step, the hydrogen peroxide reacts directly with two Cu^{2+} ions (deoxy oxidize form), forming the oxy species, necessary for catecholamine oxidation to o-quinone. At this point, the copper centers are reduced to Cu^+. An adequate potential has to

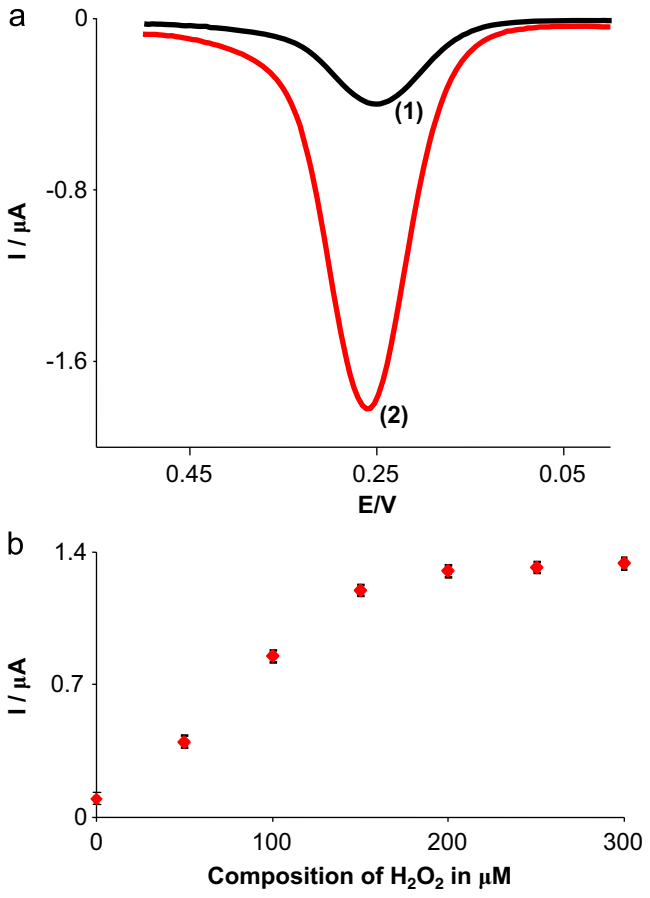

Fig. 2. (a) Square wave voltammetric response for dopamine (6.01×10^{-7} M) obtained at **1**–GCPE (1) without H_2O_2 and (2) with H_2O_2. Concentration of $H_2O_2=100\times10^{-6}$ M; pulse height 50 mV, $f=100$ Hz, $E_{acc}=+0.4$ V and $t_{acc}=40$ s in acetate buffer solution (pH 6.0). (b) A plot for the effect of concentration of H_2O_2 on the peak current of DA (3.88×10^{-7} M) **1**–GCPE employing SWV (%*RSD*=0.61).

be applied in order to allow instantaneous oxidation of Cu(I)–Cu(II) to complete the catalytic cycle. At the same time, o-quinone gets reduced to catecholamine electrochemically. Reduction of oxygen in the oxy species can be carried out by the two electrons produced during copper oxidation, which eventually leads to the formation of o-quinone and H_2O. In the next step, the catechol, which was generated electrochemically, reacts with another oxy species resulting into o-quinone and pseudo-meta tyrosinase (met form). In the met form, the copper atoms at the active site in the oxidized state (Cu^{2+}) cannot bind O_2 or H_2O_2; therefore they are inactive to catecholic substrates. Now, the electrochemical reduction of the o-quinone occurs onto the electrode surface which leads to an enhancement in the peak signal due to the cycle formed, making an analogy with the enzymatic systems for catecholamine detection. This step is considered as the most important step for quantification of phenols. The cathodic current obtained is proportional to the phenol concentration. This form is able to coordinate another molecule of catecholic substrate (met-D) and oxidize it to the o-quinone by donation of electrons to copper atoms, generating o-quinone and deoxy-reduced form (Cu_2^{2+}). Copper gets electrochemically oxidized to complete the catalytic cycle. The two electrons thus generated are used to reduce the o-quinone back to catecholamine. This step always allows the conversion of pseudo-meta species to reduced copper in order to complete the cycle. In **1**–SNP–GCPE it is expected that **1** performs the same role of the tyrosinase active site, thus enhancing the redox peak currents of DA, L-Dopa, EP and NE. This mechanism has been depicted in brief as follows:

3.4. Effect of *1* and SNP on the peak current of catecholamines

The effect of the amount of **1** and SNP to be employed as modifiers in the GCPE was first studied by varying it in the range of 1–10% with respect to glassy carbon powder (Figs. S8 and S9). It was observed that, the reduction peak current for quinone form of DA, L-Dopa, EP and NE increased with the increase in percentage of **1** and SNP up to 6% and 7%, respectively, beyond which saturation in the peak current occurred. As a result, 6% of **1** and 7% of SNP were selected as the optimum amounts for preparation of **1**–GCPE.

3.5. Cyclic voltammetry (CV)

Cyclic voltammograms of Cu(II) and **1** are given in Fig. S10. A well defined cyclic voltammogram is obtained in case of **1** as compared to that of Cu(II). Comparative cyclic voltammograms of 5.93×10^{-7} M DA, 4.34×10^{-7} M L-Dopa, 3.57×10^{-7} M EP and 4.81×10^{-7} M NE at all the four electrodes are given in Fig. S11. It can be observed that moving from GCPE to **1**–SNP–GCPE, the peak current increases for all four molecules (Fig. S11). As can be seen, a well-defined cyclic voltammogram with a considerable enhancement in the peak current is obtained at **1**–SNP–GCPE. The effective catalytic role of the **1** modified electrodes towards DA, L-Dopa, EP and NE redox peak can be attributed to the interaction between catecholamines and dinuclear copper complex in presence of H_2O_2 as given in Fig. 1(b). On the other hand, silver nanoparticles having a large electrical conductivity and a high aspect ratio enhances the peak current of catecholamines. The role of the silver nanoparticles can be understood on the basis of the fact that catecholamines exhibit an intriguing reactivity with silver nanoparticles through robust catecholamine–Ag interactions (Lin et al. 2011). Thus, a synergistic effect of **1** and SNP gives the maximum enhancement in cyclic voltammetric signal at **1**–SNP–GCPE.

As can be seen, in the cyclic voltammetry of DA (a catecholamine), three oxidation peaks (O1, O2 and O3) and two reduction peaks (R1 and R2) are observed (Fig. S11). The O1 peak is due to the oxidation of catecholamine to o-quinone which is reversible in nature. However, o-quinone easily loses proton and gets converted to aminochrome (O2) via a series of chemical reactions. Aminochrome, the chemical product of o-quinone, is electrochemically active and can be reduced to leucoaminochrome, resulting in the reduction peak of R2. On the reverse scan, leucoaminochrome gets oxidized resulting in the oxidation peak of aminochrome (O2). The leucoaminochrome is further converted to 5,6-dihydroxy indole which is electroactive in nature. This indole undergoes further oxidation to give the oxidation peak O3. A probable reaction mechanism for the reduction reactions of DA is as given in Scheme S1. L-Dopa, EP and NE also follow the same reaction mechanism with one exception in the cyclic voltammogram of catecholamines (Fig. S11(c)). Herein, EP gets oxidized to epinephrinequinone which is unstable at pH 7 and therefore the peak R1 is absent in the cyclic voltammogram of EP (Yanhong et al., 2008)

Further, the effect of potential scan rate on the peak current of the four catecholamines was studied. From Figs. S12–S15, it can also be seen that the oxidation peak shifts to a more positive value and the reduction peak for all molecules shifts to the more negative values with increasing scan rates along with a concurrent increase in current. The cyclic voltammetric results indicate that the cathodic peak currents (I_p) for all the catecholamines varied linearly with the scan rate (v) ranging from 20 mV s^{-1} to 1500 mV s^{-1} (Figs. S12–S15) which implies that the reduction of DA, L-Dopa, EP and NE is kinetically controlled on **1**–SNP–GCPE.

3.6. Electrochemical impedance spectroscopy (EIS)

A discussion regarding electrochemical impedance spectroscopy has been given in the Supporting information below Fig. S16.

3.7. Chronocoulometry (CC)

A discussion regarding chronocoulometry has been given in the Supporting information below Table S4.

3.8. Determination of Michaelis–Menten parameters by chronoamperometry

Kinetic data for reduction of DA in pH 6.0 phosphate buffer (0.1 M) was obtained by using chronoamperometry (Kamin and Willson, 1980; Lakshmi et al., 2009) for **1**–SNP–CPE at a potential of +0.1 V. The results were obtained by gradually increasing the concentration of DA in the range of 0–40 μM under stirring conditions. From plot of i vs. t, the slopes for the initial 0.7 s were measured after each increment of DA. The data were then fitted with the Michaelis–Menten model, and apparent kinetic parameters viz. Michaelis constant (K_M), maximum enzyme velocity (V_{max}), turnover number (k_{cat}) and specificity constant (k_{cat}/K_M) were estimated. The same technique was employed for all the other substrates.

K_M is taken as a measure for the strength of the intermediate transition complex which is progressively converted to the final product. A large value of K_M indicates a weak binding of catecholamines (substrate) with the binding sites (**1**) while a small value indicates a strong interaction. A plot of initial rate (derived from the slope of current vs. time over the first 0.7 s of chronoamperometric measurement) vs. substrate concentration (Fig. S17) reveals that the reaction rate increases linearly at low substrate concentrations. However, at high substrate concentrations, Michaelis–Menten process is obeyed which implies an enzyme like catalytic process. The Michaelis–Menten parameters were thus determined and are given in Table 1. The turnover number (k_{cat}) of the catalyst was determined by recording the initial rate

of oxidation of substrate (50 μM) in presence of varying quantities of **1** (range: 0–600 nmol) until saturation was observed. k_{cat} was calculated employing the formula $V_{max}=k_{cat}[E]_t$. $[E]_t$ is the concentration of the active sites which is obtained from the number of active sites (E_t) within **1**. It was observed that the initial rate increased until about 244 nmol of **1** was added to substrate (Fig. S18). Since **1** is a dinuclear complex, we get $E_t=122$ nmol in 20 mL of solution which in turn gives $[E]_t$. From the kinetic parameters (Table 1), it can be seen that catalytic effect of **1** is maximum on DA. The order for catalytic effect of **1** on catecholamines under study is: DA > EP > L-Dopa > NE. The values obtained for K_M, V_{max}, k_{cat}, and k_{cat}/K_M suggest **1** is an efficient catalyst for substrates having –OH group.

Under optimal conditions, the response time (defined as the time when 95% of the steady-state current is reached) of the biomimetic sensor was obtained by chronoamperometry. The response time is found to be 5, 8, 5 and 6 s for DA, L-Dopa, EP and NE respectively. The rapid response indicates a fast mass transfer of the substrate across the **1**–SNP–GCPE.

3.9. Scanning electron microscopy (SEM)

Fig. 3 compares the morphological features of GCPE, SNP–GCPE, **1**–GCPE and **1**–GNP–GCPE using SEM. The SEM profile of GCPE (Fig. 3(a)) was characterized by a surface of non-porous spherically shaped glassy carbon powder. The SEM image of GNP–GCPE (Fig. 3(b)) shows SNPs present along with GCPE. Fig. 3(c) shows that the GCPE has been modified by **1**. Hence, the current increase at **1**–GNP–GCPE (Fig. 3(d)) as compared to GCPE is due to the perfectly spherical structure of GCPE which are modified with highly conducting SNPs and a biomimetic copper complex (**1**). Thus, a synergistic combination of both SNPs and **1** results in high sensitivity of the modified electrode for all four catecholamines.

Table 1
Apparent Michaelis–Menten parameters obtained for the reduction of DA, L-Dopa, EP and NE on **1**–SNP–GCPE.

No.	Substrate molecule	K_M (μM)	V_{max} (μA/s)	k_{cat} (min^{-1})	k_{cat}/K_M ($\mu M^{-1}\ min^{-1}$)	Response time (s)
1.	DA	4.73	4.03	0.661	0.139	5
2.	L-Dopa	5.07	3.23	0.530	0.105	8
3.	EP	4.81	3.61	0.602	0.125	5
4.	NE	5.57	2.99	0.498	0.089	6

3.10. Adsorptive stripping differential pulse voltammetry (AdSDPV)

AdSSWV was employed by studying influence of the frequency (f), accumulation potential (E_{acc}) and accumulation time (t_{acc}) on the peak current of DA (Fig. S19), L-Dopa (Fig. S20), EP (Fig. S21) and NE (Fig. S22). Keeping the E_{acc} as +0.5 V and t_{acc} as 30 s, f was optimized by employing a range of 10–120 Hz. It can be seen from Figs. S19–S22, that the peak current for DA, L-Dopa, EP and NE reached its maximum at 100, 90, 100 and 80 Hz respectively. Thus, these f values were employed for further studies. It is known that an increase in the accumulation time improves the sensitivity of determination. Hence, the effect of variation of t_{acc} was studied over a period of 0 s–60 s, employing the optimized f for each molecule and an E_{acc} of +0.5 V. From 0 to 40 s, there was a linear increase in the peak current of DA beyond which the current began to level off. This implies that the surface saturation occurs at accumulation times above 40 s. Thus t_{acc} of 40 s was selected as the optimum time at which DA can be determined with good sensitivity. Similarly, the optimized t_{acc} values for L-Dopa, EP and NE are 30, 30 and 40 s respectively. Now, keeping f as 100 Hz and t_{acc} as 40 s, E_{acc} was varied from 0 to +0.8 V. It was observed that the highest reduction peak current of DA, L-Dopa, EP and NE was obtained at **1**–SNP–GCPE when the E_{acc} was +0.4, +0.4, +0.6 and +0.6 V respectively. Thus, these

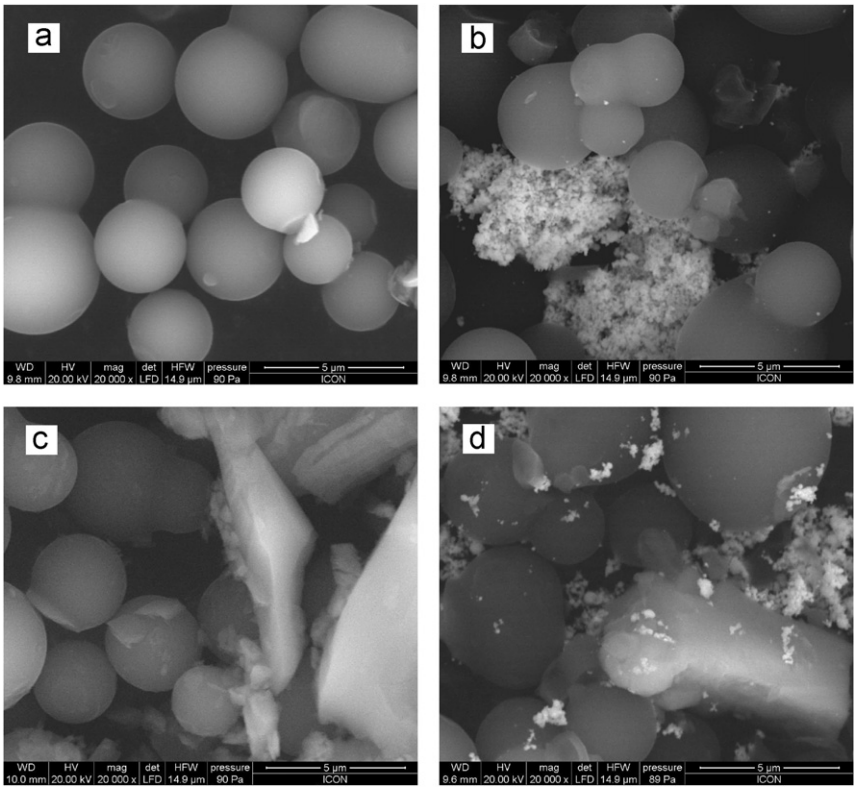

Fig. 3. SEM images of (a) GCPE, (b) SNP–GCPE, (c) **1**–GCPE and (d) **1**–SNP–GCPE.

optimized conditions were employed for AdSSWV of the four catecholamines.

Employing AdSSWV for 5.62×10^{-7} M DA, 9.75×10^{-7} M L-Dopa, 8.98×10^{-7} M EP and 7.46×10^{-7} M NE (Fig. 4), a comparative study has been carried out on GCPE, SNP–GCPE, **1**–GCPE and **1**–SNP–GCPE. It can be observed that, the best result in terms of peak current as well as peak potential is obtained in case of **1**–SNP–GCPE. As can be seen from Fig. 2(a), an enhancement in peak signal for DA was observed at **1**–GCPE only in the presence of H_2O_2 (chemical contribution to the peak current). Also, as can be seen from Fig. S19, the highest peak signal for DA was observed when +0.4 V was applied (electrochemical contribution to the peak current). Thus, the enhancement in peak current in Fig. 3 is due to dual contributions from chemical and electrochemical aspects. As can be seen from Fig. 2(a), 1–GCPE gives the maximum peak signal only in the presence of H_2O_2. Thus, it can be concluded that the electro-reduction of all these molecules becomes facile at the **1**–SNP–GCPE, therefore it was used for further studies.

Based on the above findings, an analytical method has been proposed for determining concentrations of the catecholamines employing AdSDPV at **1**–SNP–GCPE. The optimized conditions were applied for finding the limit of detection (LOD) ($S/N=3$), linear working range (LWR), linear regression equation (LRE) and correlation coefficient (r) (Table S5). For DA, a plot of i_p vs. potential (Fig. S23) was linear in the concentration range from 2.81×10^{-9} to 8.30×10^{-6} M with the LOD of 8.52×10^{-10} M while, the linear working range obtained for L-Dopa (Fig. S24) was found to be 7.77×10^{-9}–9.12×10^{-6} M with LOD of 2.41×10^{-9} M. Also, for EP, a plot of i_p vs. potential (Fig. S25) was linear in the concentration range from 1.32×10^{-9} to 8.25×10^{-6} M with the LOD of 3.96×10^{-10} M while, the linear working range obtained for NE (Fig. S26) was 1.18×10^{-9}–8.82×10^{-6} M with LOD of 3.54×10^{-10} M. Any concentration below LOD value is the residual concentration of catecholamine that remains undetected, as the analytical signal could not be differentiated from the blank signal. Also beyond LWR, saturation of the analyte onto the electrode surface limits the determination of catecholamine in the solution. The biomimetic sensor employed in the present work has advantages over enzymatic based sensors due to their short shelf life. Whereas, the copper complex used in the present work is robust in nature. Also, biosensors possess an environmental hazard while biomimetic sensors are environmentally friendly.

3.11. Interference studies, validation studies and analytical applications

In order to evaluate the selectivity of the method for the determination of DA, L-Dopa, EP and NE, the influence of potentially interfering substances on the determination of these compounds was investigated. The tolerance limit for interfering species was considered as the maximum concentration that gave a relative error less than ±5.0% at a concentration of 5.0×10^{-8} M of the four catecholamines. This data is tabulated in Table S6. This suggests that the determination of these molecules in the pharmaceutical formulations and biological samples at **1**–SNP–GCPE is not affected considerably by the common interfering species present along with the molecules of interest.

For validation of the proposed method, various parameters such as repeatability, reproducibility, precision and accuracy of analysis were obtained by performing five replicate measurements for 6.53×10^{-8}, 5.08×10^{-8}, 5.46×10^{-8} and 5.91×10^{-8} M standard DA, L-Dopa, EP and NE respectively over a single day (intra-day assay) ($n=5$) and for five days over a period of one week (inter-day

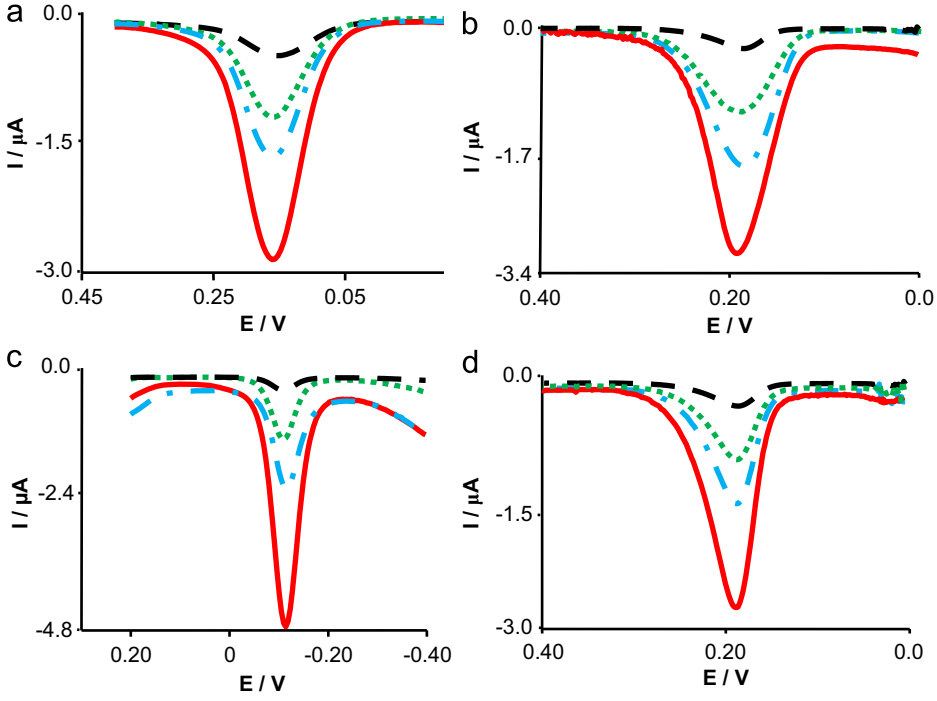

Fig. 4. Adsorptive stripping square wave voltammograms of (a) DA (3.22×10^{-7} M) at GCPE (- - -), SNP-GCPE (……), 1-GCPE (-·-·-·) and **1**–SNP–GCPE (——); pulse height 50 mV, $f=100$ Hz, $E_{acc}=+0.4$ V and $t_{acc}=40$ s in acetate buffer solution (pH 6.0); (b) L-Dopa (3.84×10^{-7} M) at GCPE (- - -), SNP–GCPE (……), **1**–GCPE (-·-·-·) and 1–SNP–GCPE (——);pulse height 50 mV, $f=90$ Hz, $E_{acc}=+0.4$ V and $t_{acc}=30$ s in acetate buffer solution (pH 6.0); (c) EP (8.98×10^{-7} M) at GCPE (- - -), SNP–GCPE (……), **1**–GCPE (-·-·-·) and **1**–SNP–GCPE (——);pulse height 50 mV, $f=100$ Hz, $E_{acc}=+0.6$ V and $t_{acc}=20$ s in phosphate buffer solution (pH 7.0); (d) NE (7.46×10^{-7} M) at GCPE (- - -), SNP–GCPE (……), **1**–GCPE (-·-·-·) and **1**–SNP–GCPE (——);pulse height 50 mV, $f=80$ Hz, $E_{acc}=+0.6$ V and $t_{acc}=40$ s in phosphate buffer solution (pH 7.0). Concentration of H_2O_2 in solution $=1.5\times10^{-4}$ M.

Table 2
Determination of DA, L-Dopa, EP and NE in pharmaceutical formulations using the HPLC method and biomimetic sensor.

No.	Molecule	Sample	[a]	[b]	[c]
1	DA	Dopar*	40	40 ± 1.2	38 ± 1.8
2		Intropin*	40	40 ± 0.77	39 ± 1.0
1	L-Dopa	Elcepam	100	98.5 ± 1.62	98.1 ± 2.33
2		Sinemet	100	99.3 ± 0.250	97.6 ± 1.23
1	EP	Adrenaline injection*	1.0	0.92 ± 0.14	0.87 ± 0.30
2		Q-Med*	1.0	0.95 ± 1.2	0.89 ± 1.4
1	NE	Adrenor*	2.0	1.9 ± 0.93	1.8 ± 1.4
2		Adrenerz injection*	2.0	2.0 ± 1.1	1.8 ± 1.7

[a] Amount of catecholamine in the sample (mg).
[b] Amount of catecholamine obtained by the proposed method (mg) ± % *RSD* ($n=5$).
[c] Amount of catecholamine obtained by the HPLC method (mg) ± % *RSD* ($n=5$).
* =mg/mL.

assay). Satisfactory mean percentage recoveries (%*R*) and relative standard deviations (%*RSD*) were obtained (Table S7). The recoveries obtained confirmed both the high precision of the proposed procedure and stability of these catecholamine solutions. The robustness of the proposed procedure (Tables S8–S11) was examined by studying the effect of small variation of pH, accumulation potential, E_{acc}, accumulation time, t_{acc} and frequency, *f*, on the recovery of the catecholamines. As can be seen from Tables S8–S11, %*R* for both the molecules were in the range of 98–102% under all variable conditions and did not show a significant change when the critical parameters were varied and hence is robust in nature. For further evaluation of the validity of the proposed method, the recovery tests for DA, L-Dopa, EP and NE in pharmaceutical formulations, urine and human serum samples were carried out as mentioned in Tables S12–S15. %*R* in the range of 97.0–01% was obtained for all the molecules. Recovery results were not affected significantly and consequently the described method is accurate for the assay of the four catecholamines in pharmaceutical formulations as well as urine and blood serum samples. For analytical applications, determinations of amount of the catecholamines in all samples have been carried out by standard addition method. The amount of all these obtained in pharmaceutical formulations agree well with the label contents. The proposed method was further validated employing HPLC. The results are as given in Table 2. It can be seen from the table that the amount of DA, L-Dopa, EP and NE obtained by the proposed method agree well with that obtained by the HPLC methods. Applying a paired *t*-test in the results obtained by this procedure and those claimed on the labels, it was found that all results are in agreement at the 95% confidence level and within an acceptable range of error. Thus, determination of these catecholamines can be carried out in various matrices by the proposed method.

3.12. Stability and reproducibility of the **1**–SNP–GCPE

A discussion regarding stability and reproducibility of **1**–SNP–GCPE is given in the Supporting information after Table S15.

3.13. Comparison of proposed method with literature methods

A comparison of the analytical performance of **1**–SNP–GCPE developed in this study with other sensors dealing with the analysis of DA, L-Dopa, EP and NE is presented in Table S16. The present method is better in terms of sensitivity as compared to all the other reported literature methods except the one given in Goyal and Bishnoi (2011) for both EP and NE determination in which the authors have employed carbon nanotubes modified edge plane pyrolytic graphite electrode. The present method is simple, does not require any pre-treatment procedure. This reveals that **1**–SNP–GCPE shows excellent analytical performance for determination of DA, L-Dopa, EP and NE in terms of wide linear dynamic range (more than three orders of magnitude), very low detection limit, high sensitivity, very good repeatability and reproducibility over other methods reported in literature.

4. Conclusion

We have synthesized and fully characterized a new dinuclear copper(II) complex (**1**) which contains an alcoholic OH group coordinated axially to each copper centers forming Cu_2O_2 non-planar ring, which mimics the intermediate proposed in the mechanism of catecholamine reduction through the enzyme tyrosinase. The ability of this complex to mimic the active site of the enzyme was successfully used to construct a biomimetic sensor. Employing **1** and SNP as modifiers in GCPE, a novel sensor has been developed for the determination of four catecholamines employing AdSSWV. Moreover, the proposed method is very sensitive having sub-micromolar detection limits for DA, L-Dopa, EP and NE. Finally, the sensor has been employed for the determination of these catecholamines in pharmaceutical formulations, urine and blood serum samples and the results are satisfactory, which suggests that **1**–SNP–GCPE can act as a promising sensor for the determination of DA, L-Dopa, EP and NE. This sensor thus has a potential for practical application in quantitative analysis of molecules possessing phenolic –OH group. Further studies are planned for developing screen-printed electrodes employing **1**–SNP–GCPE for determination of molecules possessing hydroxy groups. Also, the copper(II) complex (**1**) has a potential to be employed for trace level detection of peroxide and nitrite.

Acknowledgments

One of the authors (B.J.S.) is thankful to the Council of Scientific and Industrial Research, New Delhi, India for providing financial assistance in the form of Senior Research Fellowship (no. 09/019(0092)2K11/EMR-I).

Appendix A. Supporting information

Supplementary data associated with this article can be found in the online version at http://dx.doi.org/10.1016/j.bios.2012.07.008.

References

Babaei, A., Babazadeh, M., 2011a. Analytical Methods 3, 2400–2405.
Babaei, A., Babazadeh, M., 2011b. Electroanalysis 23, 1726–1735.
Barron, J.J., 2010. Journal of Clinical Pathology 63, 669–674.
Beitollahi, H., Sheikhshoaie, I., 2011. Journal of Electroanalytical Chemistry 661, 336–342.
Castleberry, R.P., 1997. European Journal of Cancer 33, 1430–1438.
Chirita, R.-I., West, C., Finaru, A.-L., Elfakir, C., 2010. Journal of Chromatography A 1217, 3091–3104.
Chirita, R.-I., Finaru, A.-L., Elfakir, C., 2011. Journal of Chromatography B 879, 633–640.
Claude, B., Nehmé, R., Morin, P., 2011. Analytica Chimica Acta 699, 242–248.
da Silva, Q.G., Barbosa, N.V., de Pieri Troiani, E., Faria, R.C., 2011. Electroanalysis 23, 1359–1364.
de Carvalho, M.L., Santhiago, M., Peralta, R.A., Neves, A., Micke, G.A., Vieira, I.C., 2008. Talanta 77, 394–399.
Deng, C., Chen, J., Yang, M., Nie, Z., Si, S., 2011. Electrochimica Acta 56, 8851–8856.
Diao, P., Yuan, H., Huo, F., Chen, L., Xiao, D., Paau, M.C., Choi, M.M.F., 2011. Talanta 85, 1279–1284.

ARTICLE IN PRESS

Encarnación Burgoa Calvo, M., Domínguez Renedo, O., Julia Arcos Martínez, M., 2007. Talanta 74, 59–64.
Ensafi, A.A., Khoddami, E., Rezaei, B., Karimi-Maleh, H., 2010. Colloids and Surfaces B 81, 42–49.
Fernandes, S.C., Vieira, I.C., Peralta, R.A., Neves, A., 2010. Electrochimica Acta 55, 7152–7157.
Gadhari, N.S., Sanghavi, B.J., Karna, S.P., Srivastava, A.K., 2010. Electrochimica Acta 56, 627–635.
Gadhari, N.S., Sanghavi, B.J., Srivastava, A.K., 2011. Analytica Chimica Acta 703, 31–40.
Goyal, R.N., Bishnoi, S., 2011. Talanta 84, 78–83.
Goyal, R.N., Rana, A.R.S., Aziz, M.A., Oyama, M., 2011. Analytica Chimica Acta 693, 35–40.
Hu, G., Chen, L., Guo, Y., Wang, X., Shao, S., 2010. Electrochimica Acta 55, 4711–4716.
Huang, K.-J., Jing, Q.-S., Wua, Z.-W., Wanga, L., Wei, C.-Y., 2011. Colloids and Surfaces B 88, 310–314.
Huang, S.-H., Liao, H.-H., Chen, D.-H., 2010. Biosensors & Bioelectronics 25, 2351–2355.
Jia, D., Dai, J., Yuan, H., Lei, L., Xiao, D., 2011. Talanta 85, 2344–2351.
Kamin, A., Willson, G.S., 1980. Analytical Chemistry 52, 1198–1205.
Kumar, A., Hart, J.P., McCalley, D.V., 2011. Journal of Chromatography A 1218, 3854–3861.
Kotkar, R.M., Desai, P.B., Srivastava, A.K., 2007. Sensors and Actuators B 124, 90–98.
Lakshmi, D., Bossi, A., Whitcombe, M.J., Chianella, I., Fowler, S.A., Subrahmanyam, S., Piletska, E.V., Piletsky, S.A., 2009. Analytical Chemistry 81, 3576–3584.
Li, L., Liu, H., Shen, Y., Zhang, J., Zhu, J.-J., 2011a. Analytical Chemistry 83, 661–665.
Li, Y., Liu, X., Liu, X., Mai, N., Li, Y., Wei, W., Cai, Q., 2011b. Colloids and Surfaces B 88, 402–406.
Lin, L., Qiu, P., Cao, X., Jin, L., 2008. Electrochimica Acta 53, 5368–5372.
Lin, Y., Chen, C., Wang, W., Pu, F., Ren, J., Qu, X., 2011. Chemical Communications 47, 1181–1183.
Lu, X., Li, Y., Du, J., Zhou, X., Xue, Z., Liu, X., Wang, Z., 2011. Electrochimica Acta 56, 7261–7266.
Mathiyarasu, J., Nyholm, L., 2010. Electroanalysis 22, 449–454.
Mazloum-Ardakani, M., Beitollahi, H., Sheikh-Mohseni, M.A., Naeimi, H., Taghavini, N., 2010. Applied Catalysis A 378, 195–201.
Mazloum-Ardakani, M., Ganjipour, B., Beitollahi, H., Amini, M.K., Mirkhalaf, F., Naeimi, H., Nejati-Barzokif, M., 2011a. Electrochimica Acta 56, 9113–9120.
Mazloum-Ardakani, M., Beitollahi, H., Amini, M.K., Mirkhalaf, F., Abdollahi-Alibeik, M., 2011b. Analytical Methods 3, 673–677.
Noroozifar, M., Khorasani-Motlagh, M., Akbari, R., Parizi, M.B., 2011. Biosensors & Bioelectronics 28, 56–63.
Sanghavi, B.J., Srivastava, A.K., 2010. Electrochimica Acta 55, 8638–8648.
Sanghavi, B.J., Srivastava, A.K., 2011a. Electrochimica Acta 56, 4188–4196.
Sanghavi, B.J., Srivastava, A.K., 2011b. Analytica Chimica Acta 706, 246–254.
Sanghavi, B.J., Hirsch, G., Karna, S.P., Srivastava, A.K., 2012. Analytica Chimica Acta 735, 37–45.
Shahrokhian, S., Khafaji, M., 2010. Electrochimica Acta 55, 9090–9096.
Shaikh, M.M., Srivastava, A.K., Mathur, P., Lahiri, G.K., 2009. Inorganic Chemistry 48, 4652–4654.
Shaikh, M.M., Srivastava, A.K., Mathur, P., Lahiri, G.K., 2010a. Dalton Transactions 39, 1447–1449.
Shaikh, M.M., Sanghavi, B.J., Srivastava, A.K., Mathur, P., Lahiri, G., 2010b. Analytical Chemistry 82, 5983–5992.
Sheldrick, G.M., 2008. Acta Crystallographica Section A 64, 112–122.
Sotomayor, M.D.P.T., Tanaka, A.A., Kubota, L.T., 2003a. Electrochimica Acta 48, 855–865.
Sotomayor, M.D.P.T., Tanaka, A.A., Kubota, L.T., 2003b. Electroanalysis 15, 787–796.
Švancara, I., Walcarius, A., Kalcher, K., Vytřas, K., 2009. Central European Journal of Chemistry 7, 598–656.
Van De Merbel, N.C., Hendriks, G., Imbos, R., Tuunainen, J., Rouru, J., Nikkanen, H., 2011. Bioanalysis 3, 1949–1961.
Vaze, V.D., Srivastava, A.K., 2007. Electrochimica Acta 53, 1713–1721.
Whiting, M.J., 2009. Annals of Clinical Biochemistry 46, 129–136.
Yanhong, Z., Jinquan, Y., Kangbing, W., 2008. Electrochimica Acta 53, 4615–4620.
Zhao, Y., Zhao, S., Huang, J., Ye, F., 2011. Talanta 85, 2650–2654.
Zima, J., Švancara, I., Barek, J., Vytřas, K., 2009. Critical Reviews in Analytical Chemistry 39, 204–227.

Please cite this article as: Sanghavi, B.J., et al., Biosensors and Bioelectronics (2012), http://dx.doi.org/10.1016/j.bios.2012.07.008